

Supporting Information

Figure S1/4

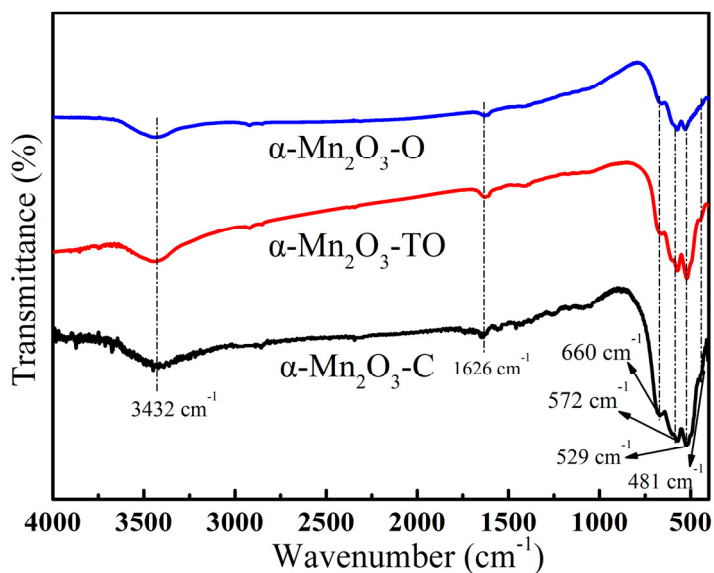


Figure S1. FT-IR spectra of $\alpha\text{-Mn}_2\text{O}_3$ catalysts with different morphologies.

Figure S2/4

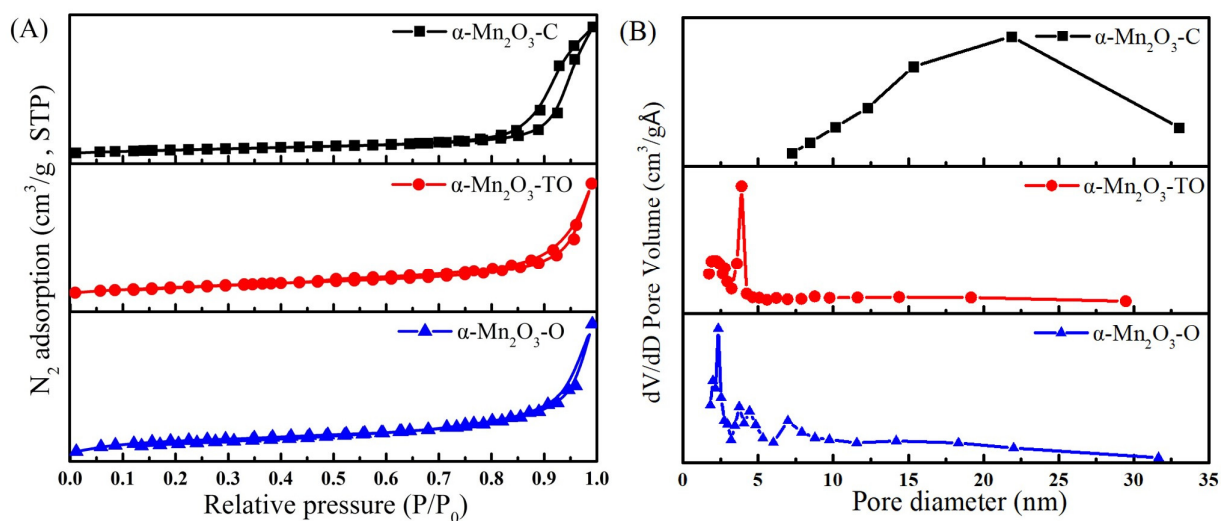


Figure S2. N_2 adsorption-desorption isotherms (A), and the pore size distributions (B) of three α - Mn_2O_3 catalysts.

Figure S3/4

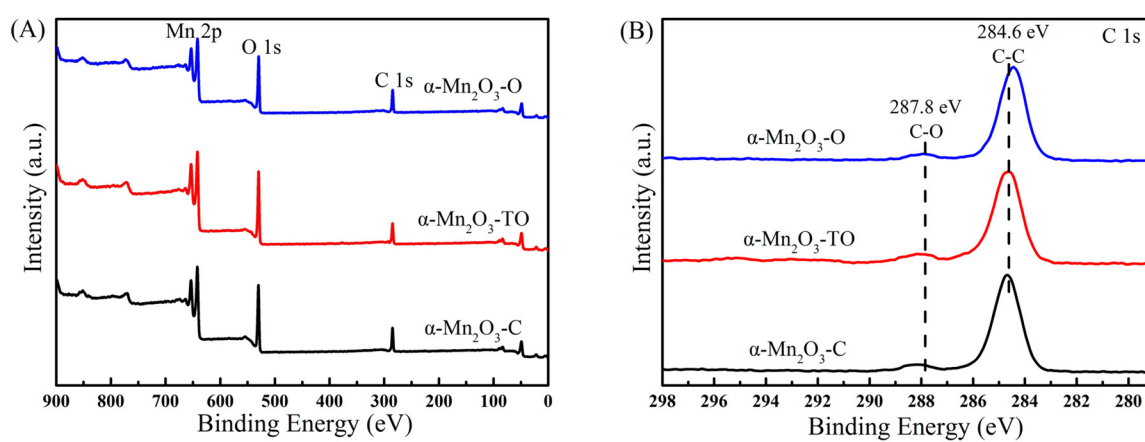


Figure S3. XPS patterns of the survey (A) and C 1s (B) of different morphologies $\alpha\text{-Mn}_2\text{O}_3$ catalysts.

Figure S4/4

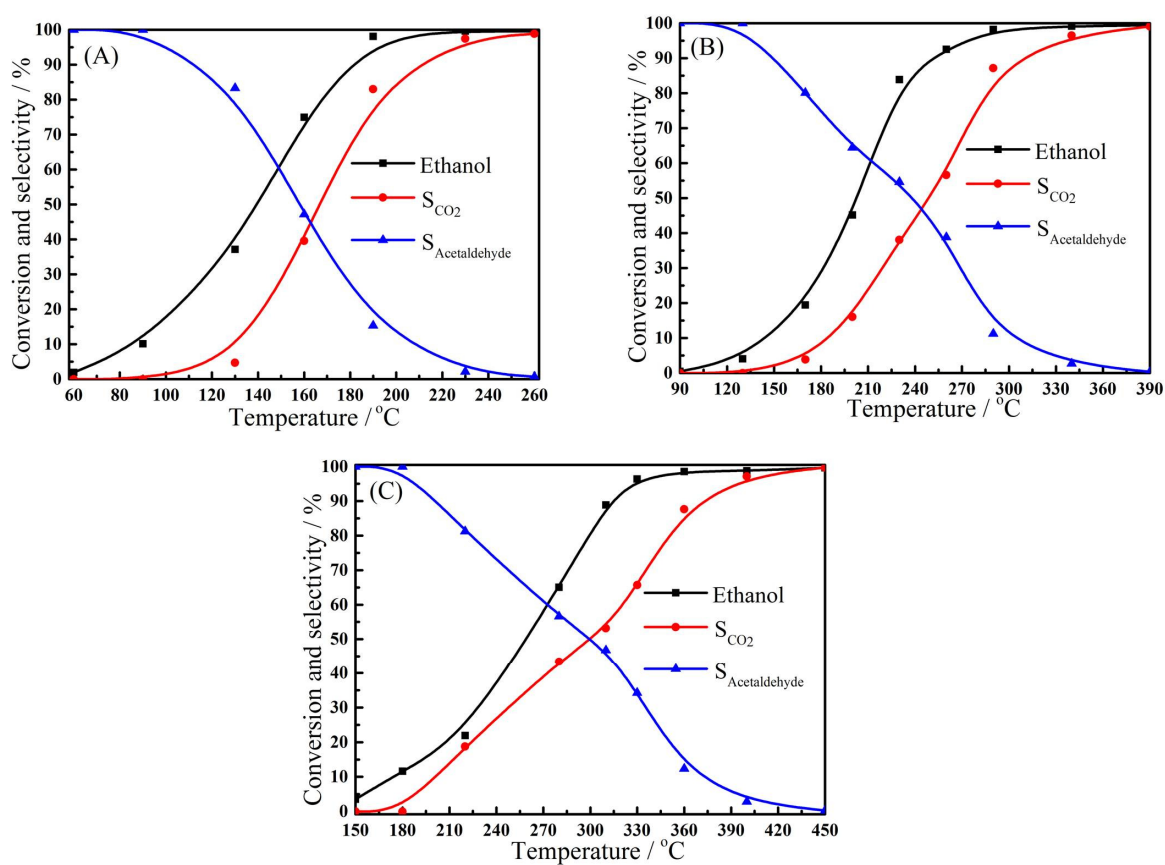


Figure S4. Ethanol conversion, acetaldehyde and CO₂ selectivity profiles of ethanol catalytic performance over $\alpha\text{-Mn}_2\text{O}_3$ catalysts with different morphologies. $\alpha\text{-Mn}_2\text{O}_3\text{-C}$ (A), $\alpha\text{-Mn}_2\text{O}_3\text{-TO}$ (B), $\alpha\text{-Mn}_2\text{O}_3\text{-O}$ (C) under normal conditions.